# Experimental observation of a topological phase in the maximally entangled state of a pair of qubits

Jiangfeng Du,[1,2,*] Jing Zhu,[1] Mingjun Shi,[1] Xinhua Peng,[2] and Dieter Suter[2]
[1]*Hefei National Laboratory for Physical Sciences at Microscale and Department of Modern Physics, University of Science and Technology of China, Hefei, Anhui 230026, People's Republic of China*
[2]*Fachbereich Physik, Universität Dortmund, 44221 Dortmund, Germany*
(Received 22 May 2007; revised manuscript received 13 July 2007; published 22 October 2007)

Quantum mechanical phase factors can be related to dynamical effects or to the geometrical properties of a trajectory in a given space—either parameter space or Hilbert space. Here, we experimentally investigate a quantum mechanical phase factor that reflects the topology of the SO(3) group: since rotations by $\pi$ around antiparallel axes are identical, this space is doubly connected. Using a pair of nuclear spins in a maximally entangled state, we subject one of the spins to a cyclic evolution. If the corresponding trajectory in SO(3) can be smoothly deformed to a point, the quantum state at the end of the trajectory is identical to the initial state. For all other trajectories the quantum state changes sign.

DOI: 10.1103/PhysRevA.76.042121 PACS number(s): 03.65.Vf, 03.67.Mn, 76.60.−k

## I. INTRODUCTION

Quantum phase factors are ubiquitous and have been crucial in explaining many phenomena that appear to be unrelated. The overall phase change resulting from the $2\pi$ rotation of a particle, e.g., distinguishes fermions from bosons or categorizes anyons [1]. If more general circuits are considered than simple $2\pi$ rotations, the states can acquire arbitrary phases even for fermions and bosons [2–4]. These phases can be split into two parts, which are referred to as dynamic and geometric. The dynamic phase is related to the energy expectation value of the quantum state, integrated over the trajectory, while the geometric part is related only to the geometry of the circuit. This analysis of quantum phases in terms of dynamical and geometrical phases was used extensively over the past decades to discuss a wide range of quantum phenomena [5].

Entanglement may well be considered to be that property of quantum mechanics that most clearly distinguishes quantum systems from their classical counterparts. It is thus extremely interesting that restricting the evolution of a quantum system to the subspace of maximally entangled states unveils a hitherto unknown type of quantum phase factor. This was shown recently by Milman and Mosseri [6,7] who considered the phase factor acquired by a pair of spins 1/2 in maximally entangled states (MESs). If one of the two spins undergoes a rotation (i.e., a local transformation), the system acquires neither a dynamical nor a geometrical phase [7], except at some points, where the overall phase of the system abruptly changes by $\pi$ [6]. These sudden changes are related to the connectedness of the space, i.e., to its topology, rather than to the geometry, i.e., its curvature [6,7].

If we consider rotations of single qubits, the appropriate space is that of the rotations in $\mathbb{R}^3$, which form a representation of the group SO(3). The total transformation of the qubit state contains, in addition to the rotation, a global phase factor, which is related to the holonomy over the trajectory in the base space SO(3) [8]. The elements of the base space can be considered to form a sphere, where the direction of each point corresponds to the orientation of the rotation axis and the distance from the origin to the rotation angle. Since rotations by $\pi$ around opposite directions are indistinguishable in $\mathbb{R}^3$ and corresponding elements of SO(3) are identical, opposite points on the surface of the SO(3) sphere have to be identified. A trajectory that crosses the surface of the sphere immediately reenters it at the opposite point. A trajectory that penetrates the surface once (or an odd number of times) cannot be smoothly deformed into one that does not cross the surface (or crosses it an even number of times). Closed trajectories can thus be classified into "plus" and "minus" classes, depending on the parity of the number of times they cross the surface. These two classes of trajectories therefore manifest the double connectedness of the SO(3) group.

This behavior can be directly mapped into the phases of the quantum states of maximally entangled spin pairs, if one of the two spins is rotated around a (possibly time dependent) magnetic field. For an arbitrary cyclic sequence $C$ of rotations of the single qubit, i.e., arbitrary trajectories in SO(3), the MES is transformed into

$$|\Psi\rangle_{\mathrm{MES}}(C) = (-1)^n |\Psi\rangle_{\mathrm{MES}}(0),$$

where $|\Psi\rangle_{\mathrm{MES}}(0)$ is the initial state and $n$ is the number of times the trajectory penetrates the surface of the SO(3) sphere. Milman and Mosseri [6] therefore call this phase a topological phase, since it is a direct consequence of the double connectedness of SO(3). In a related work, LiMing *et al.* [9] found the same behavior for trajectories where the rotation axis changes continuously. In each case, the trajectories were nonplanar, i.e., they must be considered in SO(3) and cannot be reduced to SO(2).

These papers demonstrated a connection between the topology of SO(3) (a mathematical concept) and a quantum mechanical phase factor (a physical concept). In our opinion, these new concepts call for an experimental demonstration that relates the theoretical constructs to observable phenom-

*djf@ustc.edu.cn

 

ena. This is the purpose of our paper: We report an experimental verification of this topological phase by NMR interferometry. For this purpose, we initialize a system of two nuclear spins into a (pseudo)maximally entangled state and apply radio-frequency pulses that rotate one of the two spins through trajectories that correspond either to the "+" or "−" type. In the first case, the resulting signal is identical to that of the reference system, which is not rotated, and in the second case, we observe a phase change by $\pi$. Therefore, the topological property of SO(3) is unambiguously evidenced.

The topology of SO(3) can, in principle, be explored by letting single qubits undergo the corresponding rotations. However, in this case, the resulting phase factors contain dynamical as well as geometrical contributions [10,11]. In the present context, MESs of two qubits offer a useful alternative. If we initially prepare the system in a MES and apply local transformations (i.e., rotations) to one of the two qubits, the system always remains in a MES and does not acquire any dynamical phase.

## II. TOPOLOGICAL PHASE OF MAXIMALLY ENTANGLED STATES

A general two-qubit MES can be written as

$$|\Psi\rangle = \sqrt{\frac{1}{2}}(\alpha|00\rangle + \beta|01\rangle - \beta^*|10\rangle + \alpha^*|11\rangle), \qquad (1)$$

where the coefficients $\alpha$ and $\beta$ are normalized to unity: $\alpha\alpha^* + \beta\beta^* = 1$. Without loss of generality, we choose to initialize the system in the Bell state

$$|\Psi\rangle_{\mathrm{MES}}(0) = \sqrt{\frac{1}{2}}(|00\rangle + |11\rangle) \qquad (2)$$

(i.e., $\alpha=1$, $\beta=0$), and apply the rotations to the first of the two qubits. At every point in time, we can thus identify the state of the system

$$|\Psi\rangle_{\mathrm{MES}}(t) = (U_{\hat{n}}(\theta) \otimes 1)|\Psi\rangle_{\mathrm{MES}}(0) \qquad (3)$$

with the corresponding element of SO(3). Here, $U_{\hat{n}}$ describes the unitary transformation implementing the trajectory on the first qubit and **1** is the unit operator acting on the second qubit of the MES. The unit vector $\hat{n}$ defines the overall rotation axis and $\theta$ the rotation angle, which corresponds in SO(3) to the distance from the origin.

We consider the two types of trajectories shown in Fig. 1 [7]. In each case, the first two rotations take the system from the origin (point $A$ in Fig. 1) to point $B$ and from there to point $F$. The trajectories are chosen such that $F$ corresponds to a rotation by $\pi$; it is therefore located on the surface of the SO(3) sphere and is equivalent to point $F'$ at the opposite position. From here, the + trajectory returns to the origin via point $D$, i.e., without crossing the boundary, but the − trajectory returns via $E'$. Since it "jumps" from $F$ to $F'$, the associated quantum state changes sign.

Each of the segments of the trajectories represented in Fig. 1 correspond to a rotation by $\theta=\frac{2\pi}{3}$ around one of the cube diagonal axes. Table I lists the rotation axes for each segment of both trajectories.

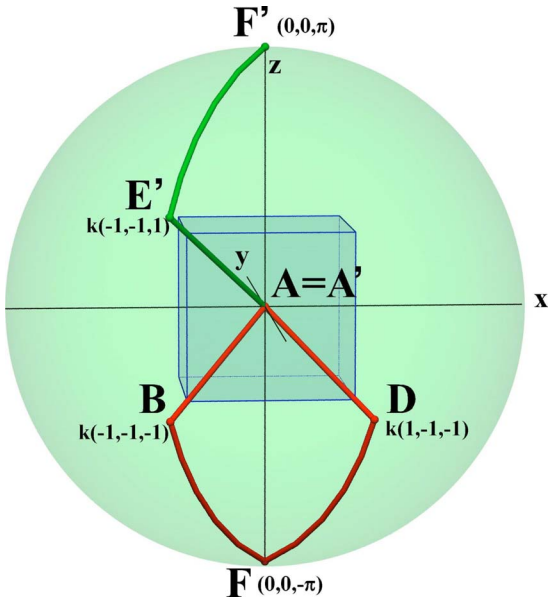


FIG. 1. (Color online) We consider two different trajectories in SO(3). The red curve $A \to B \to F \to D \to A$ belongs to the "+" class, since it does not cross the surface of the sphere. The trajectory $A \to B \to F = F' \to E' \to A'$ belongs to the "−" class. Only the second part differs from the first trajectory; it is drawn in green. $k=\frac{2\pi}{3\sqrt{3}} \approx 1.21$.

The difference between the two circuits is an overall phase factor acquired by the quantum state. Since this does not affect directly observable quantities of the system, one usually resorts to interferometric experiments for observing the sign change. Milman and Mosseri [6] suggested using optical interferometry for this purpose. Here, we resort to NMR interferometry [10].

For this purpose, we have to introduce an ancilla qubit that is coupled to the two qubits forming the MES. As shown in Fig. 2, the ancilla qubit is initialized into an equal superposition by applying a Hadamard gate to the $|0\rangle$ state. This Hadamard gate corresponds to the first beam splitter in a Mach-Zehnder interferometer. After this gate, the system is in the state

$$|\psi(0)\rangle = \frac{1}{\sqrt{2}}(|0\rangle + |1\rangle) \otimes |\Psi\rangle_{\mathrm{MES}}. \qquad (4)$$

Here, the first qubit is the ancilla qubit and qubits 2 and 3 form the MES.

TABLE I. Rotation axes of all segments of the "+" and "−" trajectories.

| + class $ABFDA$ | − class $ABF'E'A'$ |
|---|---|
| $AB: \sqrt{1/3}(-1,-1,-1)$ | $AB: \sqrt{1/3}(-1,-1,-1)$ |
| $BF: \sqrt{1/3}(1,-1,-1)$ | $BF: \sqrt{1/3}(1,-1,-1)$ |
| $FD: \sqrt{1/3}(-1,-1,1)$ | $F'E': \sqrt{1/3}(1,-1,-1)$ |
| $DA: \sqrt{1/3}(-1,1,1)$ | $E'A': \sqrt{1/3}(1,1,-1)$ |

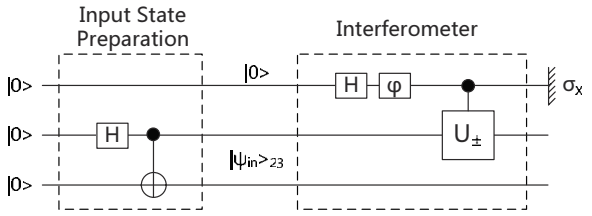


FIG. 2. Quantum network representation of input state preparation and interferometric measurement. the initial state is $|000\rangle$. $H$ is a pseudo-Hadamard gate $H=e^{-i(\pi/2)I_y}$ rotating the qubit by the angle $\frac{\pi}{2}$ about the $y$ axis, gate $\varphi=e^{-i\varphi I_z}$ rotating the qubit by the angle $\varphi$ about the $z$ axis.

Instead of the simple unitary operation corresponding to the trajectories in SO(3), we then use conditional rotations, which only act on that "copy" of the MES that is connected to the $|1\rangle$ state. After this controlled cyclic circuit, the system reaches the state

$$|\psi(cU_{\pm})\rangle = \frac{1}{\sqrt{2}}(|0\rangle \pm |1\rangle) \otimes |\Psi\rangle_{\mathrm{MES}}, \tag{5}$$

where the $\pm$ signs refer to the corresponding circuit class. If we trace over the qubits 2 and 3, we obtain the sign information by measuring the expectation value of $\langle\sigma_x^1\rangle = \pm 1$, where the sign again relates to the circuit class.

## III. EXPERIMENT

As a quantum register for these experiments, we selected the three $^{19}$F nuclear spins of Iodotrifluoroethylene ($F_2C=CFI$). This system has relatively strong couplings between the nuclear spins, large chemical shifts, and long decoherence times. The experiments were performed on a Bruker Avance II 500 MHz (11.7 T) spectrometer equipped with a QXI probe with pulsed field gradient. The resonance frequency for the $^{19}$F spins is around 470.69 MHz. The Hamiltonian of this system is (in angular frequency units)

$$H = \sum_{i=1}^{3} \omega_i I_z^i + 2\pi \sum_{i<j}^{3} J_{ij} I_z^i I_z^j, \tag{6}$$

where $I_z^i$'s are the local spin operators. The $\omega_i$ are the Larmor frequencies of the individual qubits. Relevant are the frequency differences $\omega_1 - \omega_2 \approx 12.02$ kHz and $\omega_2 - \omega_3 \approx 17.33$ kHz, and the coupling constants $J_{12}=64.2$ Hz, $J_{13}=51.3$ Hz, and $J_{23}=-129.0$ Hz.

The system was first prepared in a pseudopure state (PPS) $\rho_{000}=\frac{1-\epsilon}{8}\mathbf{1}+\epsilon|000\rangle\langle 000|$, where $\epsilon \approx 10^{-5}$ describes the thermal polarization of the system. For this initial state preparation, we used spatial averaging [12] by the pulse sequence [13].

From the input state $|000\rangle$, we prepared the maximally entangled Bell state of qubits 2 and 3 with a Hadamard and a controlled-NOT gate. The ancilla qubit 1 was then put into a superposition state by another Hadamard gate. The actual trajectories were implemented by rotating qubit 2, conditioned on the state of the ancilla qubit. If we rotate qubit 2 around the $z$ axis, conditional on the state of qubit 1, we can write the operation as

$$e^{-i\phi I_z^1 I_z^2} = \begin{cases} e^{-i(\phi/2)I_z^2} & \text{if spin 1 is in } |0\rangle, \\ e^{i(\phi/2)I_z^2} & \text{if spin 1 is in } |1\rangle. \end{cases} \tag{7}$$

Obviously, this operation can be converted into a rotation of qubit 2 by an angle $\phi$ for the case that qubit 1 is in $|1\rangle$ and no operation if it is in $|0\rangle$ if we additionally rotate qubit 2 unconditionally by $\phi/2$ around the $-z$ axis. To experimentally implement operation (7), we used

$$e^{-i\phi I_z^1 I_z^2} = e^{i\pi I_y^{1,2}} e^{-iH_d(\tau/2)} e^{-i\pi I_y^{1,2}} e^{-iH_d(\tau/2)}, \tag{8}$$

where $H_d$ is the system Hamiltonian (6) without spin 3 (this is realized by decoupling spin 3) and $\tau=\phi/(2\pi J_{12})$. A rotation around a different axis, e.g. $(-1,-1,-1)$, corresponding to the transformation $A \rightarrow B$, can be realized by sandwiching this rotation between appropriate conjugate rotations

$$R_{(-1,-1,-1)}(\phi) = R_{(-1,1,0)}(\beta) R_{(0,0,-1)}(\phi) R_{(-1,1,0)}(-\beta)$$

with $\beta=\arccos(1/\sqrt{3})$. Using these elements for the individual controlled rotations, it is straightforward to implement the full circuit. The complete pulse sequence is available in Ref. [14].

In order to improve the fidelity of these operations, we implemented the pulses as robust strongly modulating pulses (SMPs) [15–17]. We maximized the gate fidelity of the individual propagators for a suitable range of radio frequency field strengths. The theoretical fidelities over the relevant range of experimental parameters exceeded 0.995 for the individual gates, and the resulting pulse durations ranged from 200 to 500 $\mu$s. The overall theoretical fidelity of the rotations for both classes is about 0.98.

The algorithm requires the measurement of $\langle\sigma_x^1\rangle$, the $x$ component of the ancilla qubit. In a NMR experiment, this corresponds to the first point of the free induction decay (FID) In practice, better results are obtained by recording the complete FID, Fourier transforming it, and integrating the signal over the relevant frequency range.

In the experimental spectra, shown in Fig. 3, the resonance line is split into four lines by the couplings to the second and third qubits. In the figure, we have labeled the four lines with the spin states of qubits 2 and 3. While the algorithm only requires the measurement of the integrated

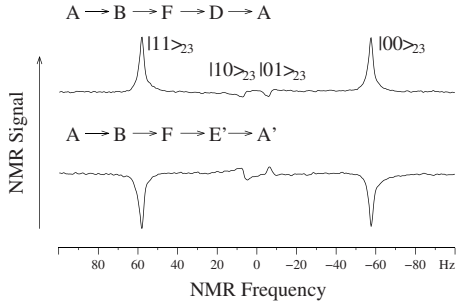


FIG. 3. $^{19}$F spectra of the ancilla qubit. The upper spectrum was obtained after the "+" trajectory was applied to qubit 2, the lower one after the − trajectory.

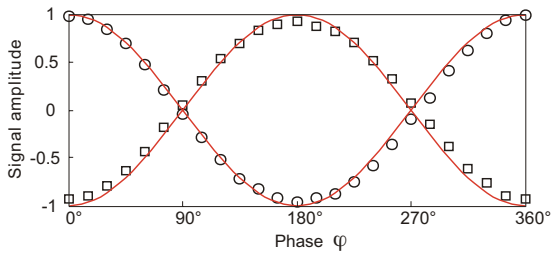


FIG. 4. (Color online) Experimental interference patterns. The squares represent the experimental data points for the "−" trajectory, the circles those of the "+" class. The lines represent the corresponding theoretical functions. Experimental data points represent integrated signal, normalized to the value for $\varphi=0$ for the "+" trajectory.

signal, the line shapes and the relative amplitudes provide useful additional information about the quality of the measurement. Ideally, the two outer resonance lines, corresponding to the states $|11\rangle$ and $|00\rangle$, should have absorption line shapes and the amplitudes should be equal; the two inner resonance lines, corresponding to $|10\rangle$ and $|01\rangle$ should vanish. Obviously, the experimental data agree well with these predictions. Small deviations are due to pulse imperfections.

The upper spectrum was obtained after applying the + trajectory (red curve in Fig. 1). In this case, the signal amplitude is positive, indicating that the trajectory did not change the phase of the quantum state. In the lower trace, we show the corresponding data after the system underwent the conditional − trajectory. In this case, the signal is inverted, as expected for a $\pi$ phase change. As an additional check that the observed sign change arises from a phase angle acquired during the trajectory, we measured a complete interferogram, by shifting the relative phase of the two states of the ancilla qubit and measuring the signal for each phase value.

Figure 4 compares the experimentally observed signal amplitudes (normalized) to the theoretical curve $\langle\sigma_x^1\rangle = \cos(\varphi-\gamma_\pm)$. $\varphi$ is the experimentally introduced phase shift, which corresponds to a delay in one arm of a Mach-Zehnder interferometer and $\gamma_\pm=\{0,\pi\}$ is the phase change due to the circuit. The agreement between the theoretical and experimental data is quite satisfactory and clearly verifies the expected phase shift of $\pi$ for the − trajectory. The experimental standard deviation $\sigma=\sqrt{\frac{1}{N}\Sigma_{i=1}^{N}(I_{\text{exp}}^i-I_{\text{th}}^i)^2}\approx 0.08$ with the experimental integral $I_{\text{exp}}^i$, the theoretical one $I_{\text{th}}^i$, and $N$ experimental points.

## IV. CONCLUSION

In conclusion, when a quantum state undergoes a cyclic trajectory, it acquires a phase factor that includes a geometrical part [2–5]. This geometrical phase is given by the total curvature of the surface enclosed by the circuit. A small variation of that circuit leads therefore, in general, to a small change of the geometrical phase.

The situation is different in the present case: small variations of the trajectory do not change the overall phase factor [9]. Instead, we only have two classes of trajectories: if the trajectory crosses the surface of the SO(3) sphere an even number of times (including 0), the total phase vanishes; if the number of crossings is odd, the state reverses its sign. The different behavior of these two classes of trajectories is directly related to the double connectedness of SO(3), and the observed phase factor may therefore be called a topological phase. A related situation is that of conical intersections [18,19], where the phase change does not depend on the area enclosed by the circuit, but only by the number of times it encircles the point of intersection. Possible extensions of this work include the investigation of multiqubit systems for different degrees of entanglement and noncyclic evolutions. These results may be relevant for topological quantum computation [20,21].

*Note added.* Recently, we became aware of two related experiments [22,23].

## ACKNOWLEDGMENTS

We acknowledge the support by National Natural Science Foundation of China, the CAS, the Ministry of Education of PRC, and the National Fundamental Research Program. This work is also supported by the DFG under contract Su 192/19-1, and by the European Commission under Contract No. 007065.

[1] F. Wilczek, Phys. Rev. Lett. **49**, 957 (1982).
[2] S. Pancharatnam, Proc. Indian Acad. Sci., Math. Sci. **44**, 247 (1956).
[3] M. Berry, Proc. R. Soc. London, Ser. A **392**, 45 (1984).
[4] Y. Aharonov and J. Anandan, Phys. Rev. Lett. **58**, 1593 (1987).
[5] A. Bohm, A. Mostafazadeh, H. Koizumi, Q. Niu, and J. Zwanziger, *The Geometric Phase in Quantum Systems* (Springer-Verlag, Heidelberg, 2003).
[6] P. Milman and R. Mosseri, Phys. Rev. Lett. **90**, 230403 (2003).
[7] P. Milman, Phys. Rev. A **73**, 062118 (2006).
[8] B. Simon, Phys. Rev. Lett. **51**, 2167 (1983).
[9] W. LiMing, Z. L. Tang, and C. J. Liao, Phys. Rev. A **69**, 064301 (2004).
[10] D. Suter, K. T. Mueller, and A. Pines, Phys. Rev. Lett. **60**, 1218 (1988).
[11] J. Du, P. Zou, M. Shi, L. C. Kwek, J.-W. Pan, C. H. Oh, A. Ekert, D. K. L. Oi, and M. Ericsson, Phys. Rev. Lett. **91**, 100403 (2003).
[12] D. G. Cory, M. D. Price, and T. F. Havel, Physica D **120**, 82 (1998).
[13] X. Peng, X. Zhu, X. Fang, M. Feng, X. Yang, M. Liu, and K. Gao, e-print arXiv:quant-ph/0202010.

[14] *Supporting Online Material: Experimental Observation of a Topological Phase in the Maximally Entangled State of a Pair of Qubits*, URL http://e3.physik.uni-dortmund.de/e3a/TopoPhase/OnlineMaterial.pdf

[15] E. M. Fortunato, M. A. Pravia, N. Boulant, G. Teklemariam, T. F. Havel, and D. G. Cory, J. Chem. Phys. **116**, 7599 (2002).

[16] M. A. Pravia, N. Boulant, J. Emerson, E. M. F. Timothy, F. Havel, R. Martinez, and D. G. Cory, J. Chem. Phys. **119**, 9993 (2003).

[17] T. S. Mahesh and D. Suter, Phys. Rev. A **74**, 062312 (2006).

[18] G. Herzberg and H. Longuet-Higgins, Discuss. Faraday Soc. **35**, 77 (1963).

[19] C. A. Mead and D. G. Truhlar, J. Chem. Phys. **70**, 2284 (1979).

[20] A. Y. Kitaev and L. Landau, Ann. Phys. (N.Y.) **303**, 2 (2003).

[21] H. Bombin and M. A. Martin-Delgado, Phys. Rev. Lett. **98**, 160502 (2007).

[22] C. Souza, J. Huguenin, P. Milman, and A. Khoury, e-print arXiv:0704.0893v1.

[23] K. Usami and M. Kozuma, e-print arXiv:0705.3155v1.